Finite-Size Berezinskii-Kosterlitz-Thouless Transition at Grain Boundaries in Solid ^{4}He and the Role of ^{3}He Impurities

Sergio Gaudio,[1,2] Emmanuele Cappelluti,[1,2] Gianluca Rastelli,[3] and Luciano Pietronero[1,2]

[1]*Dipartimento di Fisica, Università "La Sapienza", P.le A. Moro 2, 00185 Rome, Italy*

[2]*SMC Research Center and ISC, INFM-CNR, v. dei Taurini 19, 00185 Rome, Italy*

[3]*Laboratoire de Physique et Modélisation des Milieux Condensés, Université Joseph Fourier, CNRS - UMR 5493, BP 166, 38042 Grenoble, France*

(Received 28 May 2008; published 13 August 2008)

We analyze the complex phenomenology of the nonclassical rotational inertia (NCRI) observed at low temperature in solid ^{4}He within the context of a two-dimensional Berezinskii-Kosterlitz-Thouless transition in a premelted ^{4}He film at the grain boundaries. We show that both the temperature and ^{3}He doping dependence of the NCRI fraction (NCRIF) can be ascribed to finite size effects induced by the finite grain size. We give an estimate of the average size of the grains which we argue to be limited by the isotopic ^{3}He impurities and we provide a simple power-law relation between the NCRIF and the ^{3}He concentration.

DOI: 10.1103/PhysRevLett.101.075301 PACS numbers: 67.80.bd, 61.72.Mm, 68.15.+e

The report of a nonclassical rotational inertia (NCRI) in solid ^{4}He [1,2] has opened an intense debate in the physics community about its possible "supersolid" (SS) nature. Although the observation of NCRI has been confirmed by other groups [3–5], its phenomenology presents strong discrepancies with a simple supersolid phase, so that the precise origin of this phenomenon is still unclear. On one hand, the supposed SS transition appears to be anomalously broad in temperature [1–5]. On the other hand, the NCRI strongly depends on the external conditions [4–8]. In Refs. [4,6], for instance, annealing was shown to reduce and even to make disappear the NCRI fraction (NCRIF). Moreover, using a different setup, in Ref. [9] it was shown that the mass flow, associated with a SS phase, occurred only in the presence of grain boundaries (GB), and it was absent when GBs were not detected. This observation gives rise then to an alternative hypothesis to the SS phase, namely, that a liquid phase is confined at the GBs and that the mass flow is related to superfluidity of the liquid component, similarly to a Rollin film. Partial wetting of GBs was experimentally observed in Ref. [10], and the possible superfluid (SF) ordering was investigated in Refs. [11–13]. Interestingly enough, a change of the shear modulus has also been observed at low temperatures, with a similar dependence on annealing and on ^{3}He concentration as the NCRIF [14]. The connection between these two quantities is thus worth further investigation.

Quite puzzling is also the dependence of the NCRI phenomenology on the ^{3}He concentration x_3. The first report of NCRI [1] was observed in commercial ^{4}He, which contains generally a low concentration $x_3 \sim 0.3$ ppm. Further investigations showed that the critical temperature increases monotonically with x_3, whereas NCRIF increases with x_3 only up to an optimal doping at $x_3 \sim 300$ ppb, after which the magnitude decreases [15].

In this Letter we propose that, due to the strong confinement on the grain boundaries, the SF transition of the premelted liquid component can be described in terms of a two-dimensional Berezinskii-Kosterlitz-Thouless (BKT) superfluid transition where the grain size gives rise to finite size effects. We propose also a simple model where the concentration of ^{3}He impurities rules the grain size, and hence the finite size effects. We show that this framework can explain in a natural way, for $x_3 \leq 300$ ppb, the broadness of the SF transition and the dependence of the NCRIF on the ^{3}He impurity concentration.

In the following we shall model the polycrystal ^{4}He samples in terms of spherical grains with radius R and probability distribution function $P(R)$. Premelting effects, as discussed in Refs. [10–13,16], are expected to give rise to a thin liquid film with thickness d. Partial wetting [10,12], reducing the liquid amount covering the grain, can be also considered but it will not change our results. We assume that $d \ll R$, so that the liquid helium system confined on the GB surface can be regarded as two dimensional. This kind of model was employed by Kotsubo and Williams (KW) to explain the behavior of SF ^{4}He films on different substrates [17]. The important ingredient within this context is that the size R of the grain provides an intrinsic finite size cutoff which makes the BKT transition to be smooth. The broadness of the NCRI transition can be thus employed to estimate the average size R_0 of the GBs.

The BKT self-consistent equations on a spherical geometry were discussed in Ref. [17] by KW. We can define the energy $U_0(\theta)$ of an isolated vortex-antivortex pair at angular distance θ, in units of $k_B T$, as

$$U_0(\theta) = 2U_c + \int_{2\theta_c}^{\theta} \frac{\pi K_0}{\tan[(\theta' - \theta_c)/2]} d\theta', \qquad (1)$$

where $K_0 = \hbar^2 \sigma_s^0 / m^2 k_B T$ is related to the bare areal SF density σ_s^0, m is the ^{4}He mass, U_c is the vortex core energy, and $\theta_c = a_0/R$ is the minimum vortex-antivortex angular distance given by the vortex core size a_0. In the presence of screening effects due to vortex pair polarization, we can

generalize Eq. (1) as

$$U(\theta) = 2U_c + \int_{2\theta_c}^{\theta} \frac{\pi K_0}{\epsilon_0(\theta)\tan[(\theta' - \theta_c)/2]} d\theta', \quad (2)$$

where the static dielectric constant $\epsilon_0(\theta)$ can be evaluated in a self-consistent way as

$$\epsilon_0(\theta) = 1 + \frac{4\pi^3 K_0}{(2\theta_c)^4} \int_{2\theta_c}^{\theta} d\theta' \theta'^2 \sin\theta' \exp[-U(\theta')]. \quad (3)$$

Equations (1)–(3) can be evaluated self-consistently for all $\theta \leq \pi$ to obtain the observable SF density $\sigma_s(T) = \sigma_s^0/\epsilon(\theta = \pi)$ as function of temperature. Equations (1)–(3) can be also generalized to the dynamical case by introducing the dynamic dielectric constant $\epsilon(\theta, \omega)$ which depends on the diffusion constant of the vortices D and on the angular frequency ω through the parameter $r_D = \sqrt{2D/\omega}$ [17–19]. In the physical range of the experimental setup $r_D/a_0 \gg 1$ and the evaluation of the SF density σ_s in the dynamical regime is practically indistinguishable from the static one. The introduction of the dynamical analysis permits, however, the evaluation as well of the change of quality factor $\Delta[Q^{-1}]$ [17–19].

Let us now apply the above analysis to our polycrystal spherical-grain model. For a single grain of size R, assuming $d \ll R$, we can estimate the temperature dependent NCRIF $n_s(T, R)$ as

$$n_s(T, R) \simeq \frac{4\pi R^2 \sigma_s(T)}{4\pi\rho R^3/3} = \frac{3\sigma_s}{\rho R}, \quad (4)$$

(where ρ is the solid ^{4}He density), and a mean $n_s(T) = \int dR P(R) n_s(T, R)$. In the following, we shall show that the SF temperature profile is mainly ruled by the mean grain size value R_0. In this case we can roughly estimate the zero temperature NCRIF $n_s \simeq 3\sigma_s^0/\rho R_0$. Note also that in the $R_0 \gg a_0$ limit the areal SF density σ_s^0 is roughly proportional to the Berezinskii-Kosterlitz-Thouless temperature T_{BKT} where $\sigma_s(T)$ drops to zero. Within this context thus the effect of finite GB size R is mainly to give rise to a significant broadness of the transition whereas the temperature position of the drop is only weakly affected. If we assume $\sigma_s^0 \simeq \sigma_s(T_{\mathrm{BKT}}) = (2m^2/\pi\hbar^2) k_{\mathrm{B}} T_{\mathrm{BKT}}$, and we estimate T_{BKT} from the temperature T_{50} at which $n_s(T)$ drops to its 50% value of $n_s(T = 0)$, we can thus obtain a free fitting parameter estimate of the GB size:

$$R_0 \simeq \frac{6m^2}{\pi\rho\hbar^2} \frac{k_{\mathrm{B}} T_{\mathrm{BKT}}}{n_s}. \quad (5)$$

We would like to stress that, because of the simplicity of this model and of the slight approximations in the estimates of T_{BKT} and σ_s^0, Eq. (5) is simply meant to give the order of magnitude of R_0.

We now apply our model to the specific case of NCRI in solid ^{4}He. We consider a ^{4}He density $\rho = 0.2$ g/cm^3, which corresponds to a molar volume $\sim$20 cm^3 and to a pressure 41 bar. We set also typical values for the vortex core size $a_0 = 50$ Å and energy $U_c = 2.5K_0$ [20]. We consider for the moment two extreme probability distribution functions, namely, a single value $P(R) = \delta(R - R_0)$ and a flat $P(R) = 1/R_0$ for $R_0 - \Delta R_0 \leq R \leq R_0 + \Delta R_0$, with $\Delta R_0 = R_0/2$. With this choice of parameters, the overall profile of the NCRIF $n_s(T)$ is uniquely determined by the only two free parameters, namely R_0 and σ_s^0, where σ_s^0/R_0 rules the magnitude of n_s at $T = 0$ while R_0 is related to the broadness of the SF transition.

In order to show the feasibility of this approach to reproduce the experimental results, we compare in Fig. 1 the n_s vs T data for the 133 ppb ^{3}He Penn State (TOP) sample [15] with our best fit, which gives $\sigma_s^0 = 0.26 \times 10^{-9}$ g/cm^2 and $R_0 = 130$ Å, and with a infinite size BKT transition for large grains $R \gg a_0$. Note that there is only a slight difference between the δ-like and the flat $P(R)$. As a matter of fact, we have checked that different distribution functions $P(R)$ do not affect qualitatively our results, so that from now on we shall consider for simplicity a simple δ-like distribution. The nice agreement between the experimental data and our results suggests that the NCRI broad transition is not related to inhomogeneities of the samples but it stems from finite size effects due to the finiteness of the ^{4}He grain. It is important to underline that, while the fitting procedure gives a refinement of the GB size, the order of magnitude of R is essentially given by the relation (5), so that the good agreement in the broadness of the transition is not a result of the fit but it can be considered as an independent check of the validity of our analysis.

The estimate size $R_0 \simeq 130$ Å of the grains can appear quite puzzling especially considering that ^{4}He at these conditions is thought to solidify in a polycrystal form with macroscopic size of grains. However, on one hand the crystallographic evidence cannot esclude mosaics of small-angle grain boundaries. On the other hand, the presence of such small grains can naturally account for the high sensitivity to annealing and to preparation and freezing procedures, and the similarities with the NCRI phenomenology in Vycor glasses [21]. Nevertheless, the physical origin of such an extremely small grain size and its dependence on ^{3}He concentration requires explanation. We address this issue in the second part of this Letter, where we

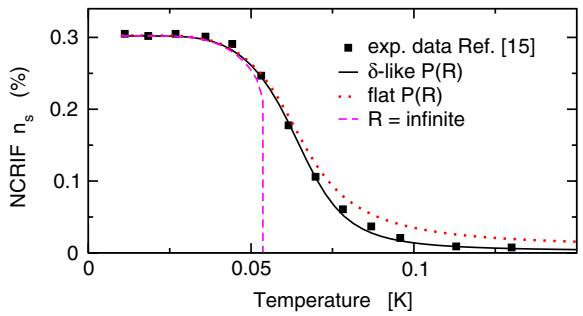

FIG. 1 (color online). Comparison between experimental data for the 133 ppb TOP sample (symbols) [15] and our theoretical analysis. Also shown is the BKT curve for $R = \infty$.

relate the origin of GB to the presence of liquid melted bubbles induced by ^{3}He impurities.

In order to gain a further insight on this point, let us discuss before the experimental dependence of the NCRI phenomenology on the He^3 concentration and on the growth or measurement condition. In particular, we analyze two samples [15] in the highly dilute limit $x_3 \simeq 1$ ppb, one belonging to the University of Florida (TOF) family, grown with the blocked capillary method, and one still belonging to the Penn State University but grown at constant pressure (CP). For both these samples measurements of the change of the quality factor $\Delta[Q^{-1}]$ were also available [15].

The first thing to observe is that, despite both samples are at same x_3, the signals are significantly different (Fig. 2). For the TOF sample, the value of n_s is almost 1 order of magnitude smaller than for the CP sample. Its variation as a function of the temperature is also different. In fact, while the n_s presents a quite smooth behavior in the CP sample, the drop of n_s at $T \simeq 0.03$ K is much sharper followed by an additional tail. Similar features are observed in the behaviors of the quality factor $\Delta[Q^{-1}]$, which is quite broad in the CP sample compared to the sharp peak at $T \simeq 0.03$ K in the TOF sample [note that the longer tail in the n_s is not observed in $\Delta[Q^{-1}]$, suggesting that this features in the $n_s(T)$ behavior could have a spurious origin].

We can see now that our model permits an understanding, in a very natural way, also the x_3 dependence of the NCRI phenomenology. We first note that, although the two samples have different $n_s(T = 0)$ of a order of magnitude, their T_{BKT}, defined for instance as $T_{\mathrm{BKT}} = T_{50}$, are of a similar magnitude. A simple analysis, using again Eq. (5), would point out thus an average radius R_0 of the GBs in the TOF sample 1 order of magnitude larger than in the CP one. As a consequence, finite size effects are expected to give rise to a much sharper transition in the TOF than in the CP case, in agreement with the experimental observation. These simple considerations are corroborated by a more detailed analysis. In Fig. 2 we show our best fits for both the TOF and CP samples, compare with the experimental data. Estimates for R_0 and σ_0, in these cases, are, respectively, $R_0 = 790$ Å, $\sigma_s^0 = 0.105 \times 10^{-9}$ g/cm^2, and $R_0 = 100$ Å, $\sigma_s^0 = 0.216 \times 10^{-9}$ g/cm^2. For the evaluation of the quality factor $\Delta[Q^{-1}]$ we have used, respectively, $r_D = 1.2 \times 10^4$ Å and $r_D = 0.3 \times 10^4$ Å, which give $r_D/R \gg 1$. We remind that in such a quasistatic regime, the parameter r_D simply acts as a scale factor on $\Delta[Q^{-1}]$ while it does not affect significantly the NCRIF. The reliability of such a limit is confirmed by Ref. [5], where the magnitude of $\Delta[Q^{-1}]$ was shown to be sensibly affected by changing the setup frequency while the NCRIF was essentially untouched.

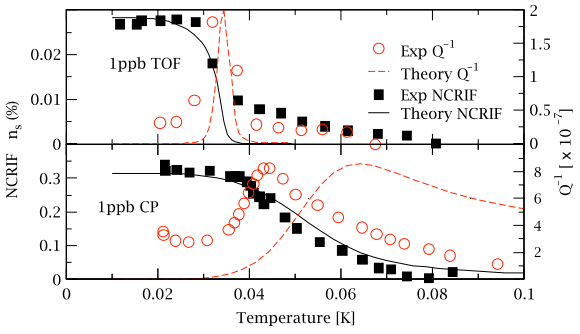

FIG. 2 (color online). Comparison between theory and experimental NCRIF and $\Delta[Q^{-1}]$ data taken from Ref. [15] for the 1 ppb TOF (upper) and CP (lower) samples.

We can see that the finite GB size BKT theory can naturally account not only for the broad NCRIF transition but also for the experimental height and broadness of the $\Delta[Q^{-1}]$ factor. This latter point is not surprising since in the finite size BKT framework, the broadness of the n_s transition and of the $\Delta[Q^{-1}]$ peak are related. Although our theory can account for the difference of the signals in a simple manner, the long tail of n_s for $T > T_{\mathrm{BKT}}$ in the TOF sample remains unexplained. As mentioned above, however, it should be noted that this feature of the NCRIF has no counterpart in $\Delta[Q^{-1}]$, which is sharply located at $T \approx T_{\mathrm{BKT}}$ [15]. This suggests that the long tail in $n_s(T)$ might be due in this sample to different physics not related to the superfluid GB transition.

After we have assessed the robustness of our analysis in explaining the NCRI phenomenology as function of x_3 and growth conditions, in the last part of this Letter we address the origin itself of such x_3 dependence. In particular, we propose that the main effect of ^{3}He impurities is to provide an intrinsic maximum length scale for the growth of grains, favoring thus the presence of grain boundaries, and hence to sustain a superfluid NCRI on the GB surfaces. It should be clear, on the other hand, that additional sources of disorder, favoring the GB formation, can be present, as shown by the different phenomenology for different growth conditions and by the annealing dependence [4,6]. We assume for the moment that the only source of GB is the presence of ^{3}He impurities. This assumption is probably valid for the TOF samples, which show the smallest NCRIFs for similar x_3, and it is corroborated by the sharp drops of n_s at T_{BKT}, suggesting quite large grains. We consider, for dilute ^{3}He concentrations $x_3 \lesssim 1$ ppm, a uniform distribution of the ^{3}He impurities within the sample, with an average distance $d_{^3\mathrm{He}}$ between ^{3}He atoms $d_{^3\mathrm{He}} \approx x_3^{-1/3}$. In Ref. [16] it was shown that ^{3}He impurities, due to the stronger quantum fluctuations of zero point motion, induce a local melting of the host ^{4}He even at low temperature much smaller than the bulk ^{4}He melting. The presence of local liquid spots, which we remind survive also at virtually zero temperature around the ^{3}He impurities, poses a strong constraint on the growth of the grain size in the freezing process. The average distance $d_{^3\mathrm{He}}$ provides thus the maximum length scale for the growth of grain size and, in the last analysis, an average value of the grain diameter $2R_0 \simeq d_{^3\mathrm{He}}$ [see Fig. 3(a) for a sketched

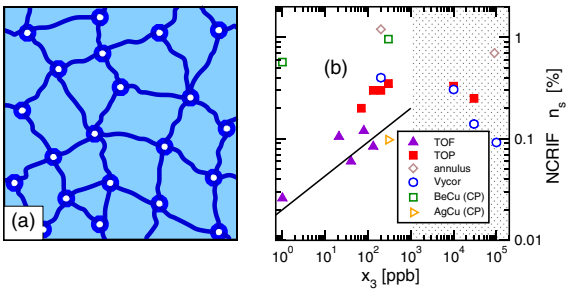

FIG. 3 (color online). (a) schematic sketch of GB structure of ^{4}He samples in the presence of ^{3}He impurities. Light blue areas represent solid ^{4}He, white spots ^{3}He impurities and dark blue regions premelted ^{4}He at the GBs and around ^{3}He impurities. (b) n_s vs x_3 plot of different samples (symbols) taken from Ref. [15] compared with our model prediction [Eq. (6)] (solid line), which is expected to fail in the gray region where $R \gtrsim 2 - 3a_0$ and the mean-field theory breaks down.

picture). This simple estimate gives for instance $R_0 \simeq 1600$ Å for $x_3 = 1$ ppb and $R_0 \simeq 313$ Å for $x_3 = 133$ ppb, 2–3 times larger than the actual fit estimates. Taking into account that these figures are purely indicative since other sources of disorder are always present further limiting the size of the grains, such estimates are not bad and provide the order of magnitude of the grain size. The most convincing probe of such a picture is the power-law dependence of the behavior of n_s as function of x_3, $n_s \approx x_3^{1/3}$. Assuming that a p_s fraction of the thin liquid film of thickness d at the GBs undergoes a superfluid BKT transition, and approximating the liquid ^{4}He density with the solid one, we have an areal SF density at the GBs $\sigma_s = p_s d\rho$, and, from Eq. (4),

$$n_s \approx 6p_s d/d_{^3\mathrm{He}} \approx 6p_s d x_3^{1/3}/a, \qquad (6)$$

where we have assumed $d \ll R_0$ and $R_0 \approx d_{^3\mathrm{He}}/2$. where $a = 3.2$ Å is the solid He-He distance at the pressure here considered. Such power-law behavior, assuming for instance $d = 1.2$ Å and $p_s = 0.01$, is shown in Fig. 3(b) in qualitative agreement with the experimental data for the TOF samples and the lowest x_3 TOP samples [15] where other sources of disorder are thought to be small. Note that the unknown quantities p_s, d, in the log-log plot of Fig. 3 (b), determine only the vertical off-shift of the $\log n_s - \log x_3$ behavior but not its slope which is uniquely determined by geometrical considerations. In CP samples on the other hand additional limiting mechanisms on the grain size are probably operative concealing the ^{3}He effects. This is in agreement indeed with the larger values of n_s and with the broader drops of NCRIF [5,15]. The validity of this analysis is in addition limited by the mean-field character of our approach. For $x_3 \gtrsim 10^3$ ppm the average size of the grains is predicted to be $R_0 \lesssim 150$ Å, only 2–3 times larger than the vortex size $a_0 = 50$ Å. In this regime the reliability of the mean-field analysis is strongly questionable.

In conclusion, in this Letter we showed that the complex NCRI phenomenology is fully compatible with a superfluid Berezinskii-Kosterlitz-Thouless transition induced in the thin premelted liquid film at the grain boundaries. Note by the way that the two-dimensional BKT transition is characterized by the lack of specific heat anomalies, in agreement with the heat-capacity measurements in solid ^{4}He [22–24]. Both the temperature and x_3 dependence are shown to be ascribable to finite grain size effects. We propose also a simple picture where ^{3}He impurities are directly related to the maximum size of the grains and we predict a simple scaling relation between the NCRIF n_s and the ^{3}He impurity concentration.

We acknowledge useful discussions with J. Beamish, H. Alles, A.V. Balatsky. M. Holzmann, S. Balibar, and F. Caupin.

[1] E. Kim and M. H. Chan, Nature (London) **427**, 225 (2004).
[2] E. Kim and M. H. Chan, Science **305**, 1941 (2004).
[3] M. Kondo *et al.*, J. Low Temp. Phys. **148**, 695 (2007).
[4] A. S. C. Rittner and J. D. Reppy, Phys. Rev. Lett. **97**, 165301 (2006).
[5] A. S. C. Rittner, J. C. Graves, and H. Kojima, Phys. Rev. Lett. **99**, 015301 (2007).
[6] A. S. C. Ritter and J. D. Reppy, Phys. Rev. Lett. **98**, 175302 (2007).
[7] E. Kim and M. H. W. Chan, Phys. Rev. Lett. **97**, 115302 (2006).
[8] A. C. Clark, J. West, and M. H. W. Chan, Phys. Rev. Lett. **99**, 135302 (2007).
[9] S. Sasaki *et al.*, Science **313**, 1098 (2006).
[10] S. Sasaki, F. Caupin, and S. Balibar, Phys. Rev. Lett. **99**, 205302 (2007).
[11] N. Prokof'ev and B. Svistunov, Phys. Rev. Lett. **94**, 155302 (2005).
[12] L. Pollet *et al.*, Phys. Rev. Lett. **98**, 135301 (2007).
[13] M. Rossi *et al.*, arXiv:cond-mat/0707.4099.
[14] J. Day and J. Beamish, Nature (London) **450**, 853 (2007).
[15] E. Kim *et al.*, Phys. Rev. Lett. **100**, 065301 (2008).
[16] E. Cappelluti *et al.*, Phys. Rev. B **77**, 054301 (2008).
[17] V. Kotsubo and G. A. Williams, Phys. Rev. Lett. **53**, 691 (1984); Phys. Rev. B **33**, 6106 (1986).
[18] V. Ambegaokar, B. I. Halperin, D. R. Nelson, and E. D. Siggia, Phys. Rev. B **21**, 1806 (1980).
[19] C. Wang and L. Yu, Phys. Rev. B **33**, 599 (1986).
[20] H. Cho and G. A. Williams, Phys. Rev. Lett. **75**, 1562 (1995).
[21] D. Ceperley, Nature Phys. **2**, 659 (2006).
[22] J. Day, T. Herman, and J. Beamish, Phys. Rev. Lett. **95**, 035301 (2005).
[23] J. Day and J. Beamish, Phys. Rev. Lett. **96**, 105304 (2006).
[24] I. A. Todoshchenko *et al.*, Phys. Rev. Lett. **97**, 165302 (2006).